Hindawi
Journal of Advanced Transportation
Volume 2018, Article ID 6376417, 9 pages
https://doi.org/10.1155/2018/6376417

WILEY | Hindawi

Research Article

Waypoint Position Optimization for Accurate Ground-Based Arrival Time Control of Aircraft

Noboru Takeichi

Department of Aeronautics and Astronautics, Tokyo Metropolitan University, 6-6 Asahigaoka, Hino, Tokyo 191-0065, Japan

Correspondence should be addressed to Noboru Takeichi; takeichi@tmu.ac.jp

Received 16 October 2017; Accepted 3 June 2018; Published 28 June 2018

Academic Editor: Yuchuan Du

In the ground-based arrival time control operation, the measurement of the arrival time error and the speed advisory to cancel it are performed at specific waypoint(s). It is generally recognized that the arrival time accuracy depends on the accuracy of trajectory prediction and control and the availability of information about the aircraft intent. Additionally, the position of the waypoint also determines the arrival time accuracy. Therefore, in this study, the feasibility of waypoint position optimization to improve the arrival time accuracy of aircraft controlled by ground-based speed advisory and its effectiveness are discussed. The models of flight time uncertainty and the arrival time control window were developed using the actual track and numerical weather forecast data. An optimization problem was formulated that defined the arrival time uncertainty at the terminal point as the objective function and numerically solved using sequential quadratic programming. Through numerical investigations, the feasibility of the waypoint position optimization and its effectiveness were clearly demonstrated in comparison with uniform arrangement cases. It was also clarified that the advantage of the multiple waypoint application was enhanced when larger arrival time control windows were available.

1. Introduction

In future air traffic plans [1–3], civil aviation authorities plan to introduce a time-based operation to manage the increase of air transportation demand. Arrival management (AMAN) is recognized as one of the promising applications of a time-based operation. In the original AMAN concept [4, 5], aircraft descend from the cruise altitude to reach the merging point placed near an airport, for example, the runway threshold, and the waypoint at an intermediate altitude at each aircraft's required time to achieve efficient time separation. The required time to arrive at the merging point is determined by air traffic controllers (ATCs) based on the estimated time of arrival (ETA) of aircraft in the same traffic stream. Aircraft equipped with required time of arrival (RTA) functionality can satisfy this using the airborne control [6]. However, not all aircraft are equipped with RTA functionality, and, in particular, fewer aircraft are equipped with it for descent trajectories [6]. For an aircraft incapable of the RTA functionality on a descent trajectory, it is necessary for the ground controllers to estimate its arrival time from its state and indicate the airspeed to satisfy the required time to arrive for an appropriate separation from the preceding aircraft. Additionally, as an increase of unmanned air systems is expected [7, 8], it is possible that the need for ground-based trajectory management will increase.

Numerous studies concerning ground-based trajectory management have been devoted to clarifying its feasibility [9–15] and improvement of operability [16–19], efficiency [20, 21], and accuracy [22–24]. Among the studies on accuracy improvement, the improvement of wind prediction accuracy [22, 24] and ground use of flight intent [23] have often been the focus. Despite the fact that the position of the waypoints used to measure the time to arrive and determine the flight speed to satisfy the required time are also expected to affect the arrival time accuracy, conventional waypoints have been applied in the aforementioned past studies. Although the application of multiple waypoints has been introduced to improve the arrival time accuracy [14], only conventional waypoints have been used. Even in a recent study on the application of the ground-based speed advisory [25], the waypoints were evenly spaced. Thus, no studies have been

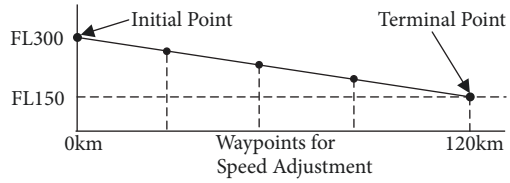

Figure 1: Flight route for analysis.

conducted on the optimum positions of the waypoints to improve the accuracy of ground-based arrival time control.

In this study, we aim to clarify the feasibility of waypoint position optimization to improve the arrival time accuracy of ground-based arrival time control. For this purpose, the uncertainty model of the ground-based trajectory prediction is derived using actual operation data and weather forecast data. Additionally, the arrival time control window models using the speed advisory are also derived. Through numerical analysis using these models, the feasibility of the optimum waypoint position and its effectiveness are investigated. The waypoint optimization is extended for the application of multiple waypoints, and its effectiveness is clarified.

Flight trajectories to Tokyo from the westward direction are particularly focused on in this study because they represent the heaviest traffic in Japan. The descent trajectory under consideration is shown in Figure 1. Aircraft continuously descend from the initial point at an altitude of 30,000 ft to the terminal point placed 120 km away at an altitude of 15,000 ft. This trajectory was determined to imitate the flight path angle of the actual descent trajectories toward Tokyo presented in the next section. The following sequence of the arrival time control operation is considered: (1) before departure, the pilot enters the descent route parameters including the optimized positions of waypoints into the Flight Management System; (2) before arriving at the initial point, the pilot is provided with a constant indicated airspeed (IAS) by the ATC to satisfy the required time to arrival at the terminal point; (3) at the moment of passing through the waypoints, the flight time error is measured and the ATC newly calculates a constant IAS to meet the indicated required time to arrive; and (4) the pilot receives the calculated IAS and immediately adjusts the IAS to the received IAS using Mode Control Panel.

2. Track and Weather Data

In this study, the secondary surveillance radar (SSR) Mode S [25] data measured at the ground station in a Tokyo suburb were used for analysis. The following data were provided [26]: clock, aircraft identifier and type, longitude and latitude, pressure altitude, true track angle, ground speed (GS), magnetic heading, true airspeed (TAS), and IAS. Aircraft data within 250 NM from the ground station were provided once every 10 s. The SSR Mode S data acquired from December 1 to 31, 2014, were selected for analysis. The aircraft trajectories toward Tokyo were extracted by limiting the heading angle from 60 to 100 degrees in the area in which the latitude was below N35 deg. As aircraft usually maintain their IAS during descent, the flight segment data with almost constant IAS, where its moving average was below 0.1 kt/s and no continuous acceleration or deceleration longer than 30 s was recorded, were extracted as the typical operation trajectories. Their lateral and vertical paths and the relationship between the IAS and altitude are shown in Figure 2. The total number of extracted trajectories was 3,084.

The wind forecast data were provided as the grid point value of the numerical weather forecast data by the Japan Meteorological Agency [27]. This model was developed to precisely predict the weather around the Japanese territory. The wind vector and temperature data were provided every 3 hours, containing every 0.1 degrees in both longitude and latitude. In the analysis, the wind forecast data were applied using linear interpolation.

3. Flight Time Uncertainty Model

The flight time error arises from the difference between the intent GS and actual GS. The actual GS was provided in SSR Mode S data. However, no information concerning the flight intent was provided. In a time-based operation, the intent GS is determined according to the required arrival time, the intent TAS is determined according to the intent GS and forecast wind speed, and the intent IAS is calculated from the intent TAS. Therefore, in this study, the intent GS was estimated from the IAS recorded in SSR Mode S data and weather forecast data. Because the aircraft in descent phases toward a destination airport was inferred to maintain a constant IAS, as mentioned above, the intent IAS was determined as the average IAS of each trajectory. Then, the intent IAS was translated into the intent TAS using the forecast temperature and pressure [28]. The intent GS was estimated as the sum of the intent TAS and the forecast wind speed in the flight direction. Finally, the flight time error for a certain distance D was obtained as

$$T_{err} \triangleq T_{act} - T_{int}, \tag{1}$$

where

$$\int_0^{T_{act}} GS_{act}\,dt = D \tag{2}$$

and

$$\int_0^{T_{int}} GS_{int}\,dt = D. \tag{3}$$

To imitate the descent trajectory shown in Figure 1, the 657 trajectories that initiated descent with near constant IASs above the altitude of 30,000 ft, as shown in Figure 3, were extracted for the flight time uncertainty modeling. An example time-history of the flight time error of an example trajectory is shown in Figure 4. The horizontal axis shows the flight distance obtained as the time integration of actual and intent GSs, and the vertical axis shows the flight time and its error obtained as their difference. The mean and standard deviations (STDs) and the root mean square (RMS) were calculated at every 20 km and summarized in Figure 5 and Table 1. The example flight time error histogram at a

Table 1: Summary of the mean deviation, STD, and RMS.

Distance [km]	Num. of Samples	Mean Dev. [s]	STD [s]	RMS [s]
20	657	1.28	3.09	3.34
40	532	2.51	6.19	6.68
60	435	3.93	9.53	10.3
80	372	5.04	13.94	14.81
100	289	5.14	18.07	18.75
120	151	4.24	20.64	21.00

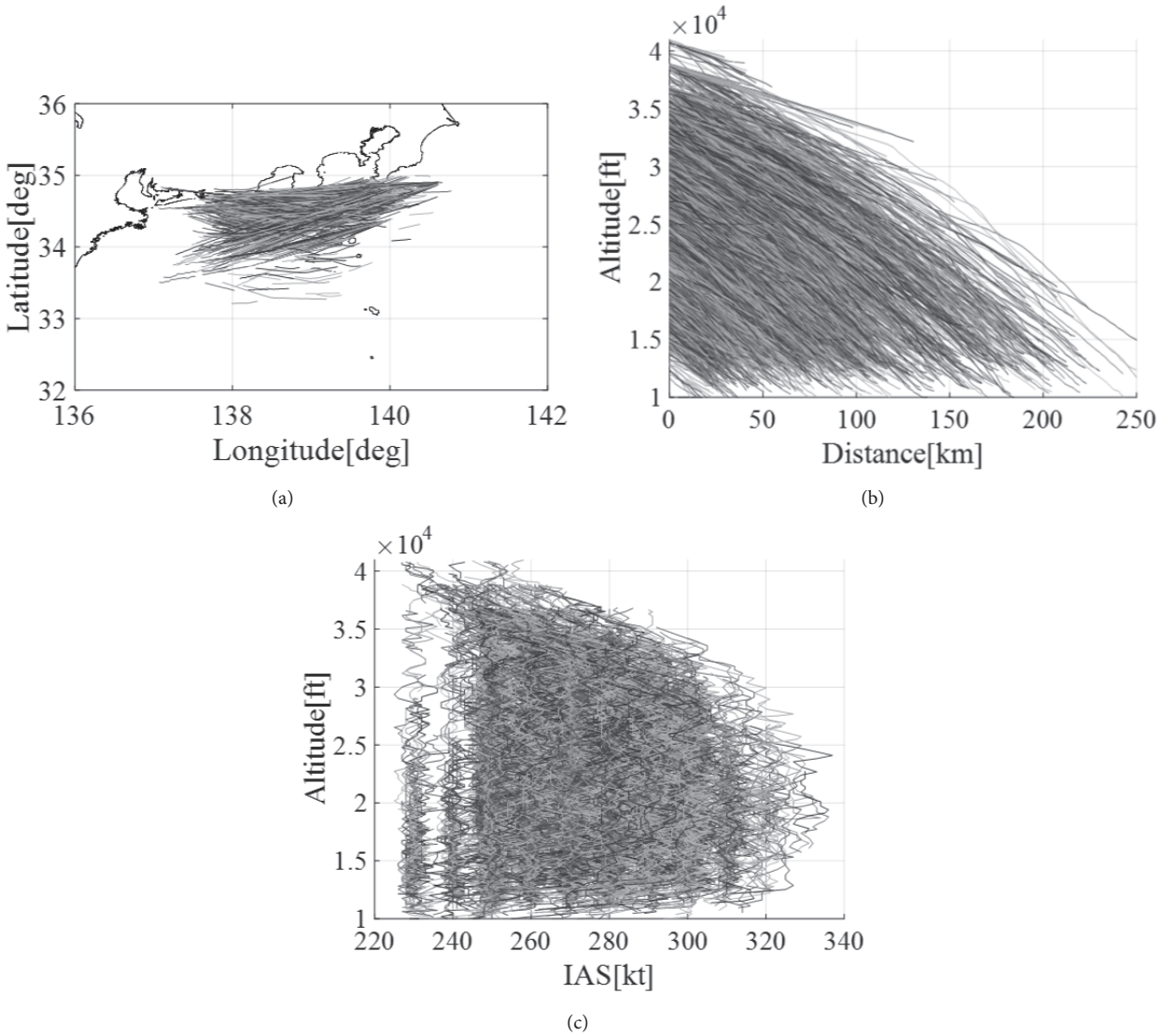

Figure 2: Extracted trajectories: (a) lateral path, (b) vertical path, and (c) IAS altitude.

distance of 40 km is shown in Figure 6, which shows that the flight time error distribution is mound-shaped and slightly biased. Because the actual data were processed, the mean values could never become exactly zero, even though they were rather small. Therefore, in this study, the RMS value was regarded as the measure of the flight time uncertainty. It is obvious that the RMS value was almost linearly proportional to the flight distance. Its approximate function was obtained as follows:

$$\sigma(D) = 1.95 \times 10^{-4} D\,[\text{sec}], \tag{4}$$

where $D[m]$ is the flight distance. Thus, the flight time uncertainty model was obtained as a function of the flight distance.

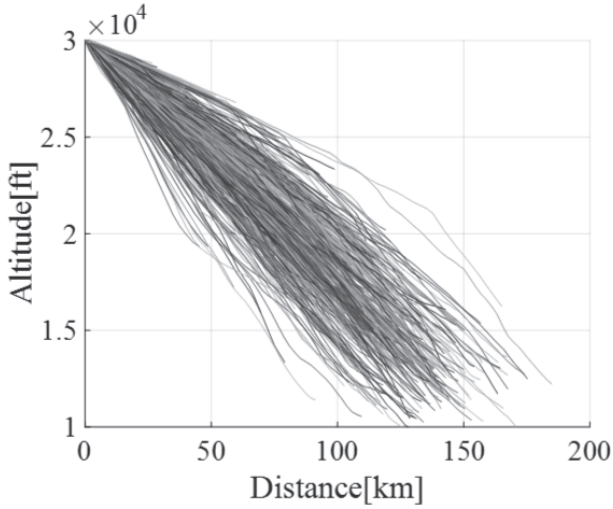

Figure 3: Vertical profiles of extracted paths from an altitude of 30,000 ft.

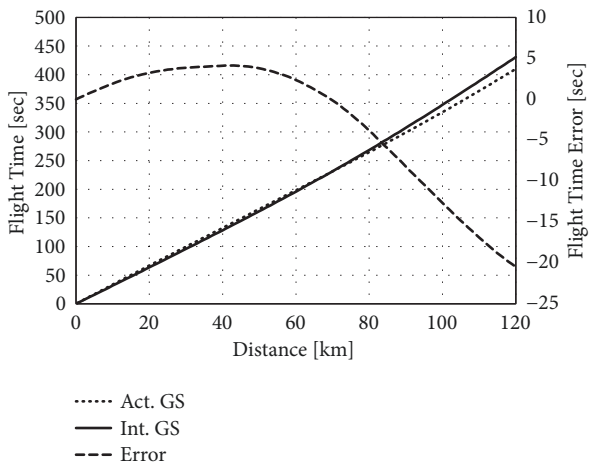

Figure 4: Example of the flight time error calculation.

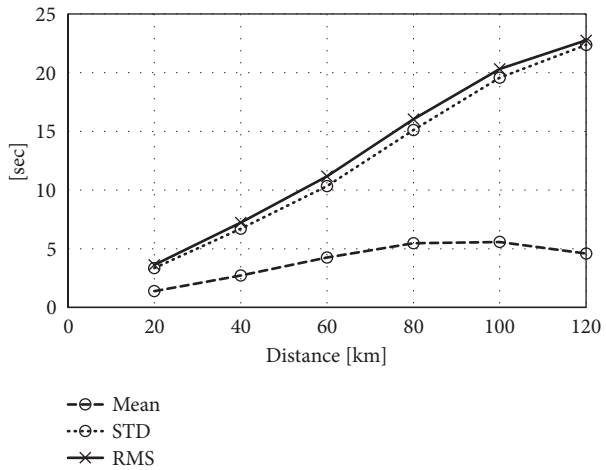

Figure 5: Mean deviation, STD, and RMS of the flight time error.

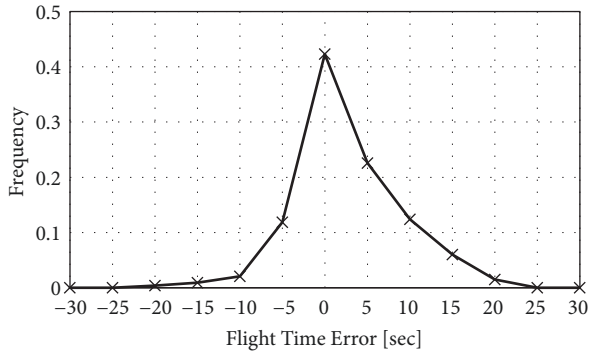

Figure 6: Histogram of the flight time error at 40 km.

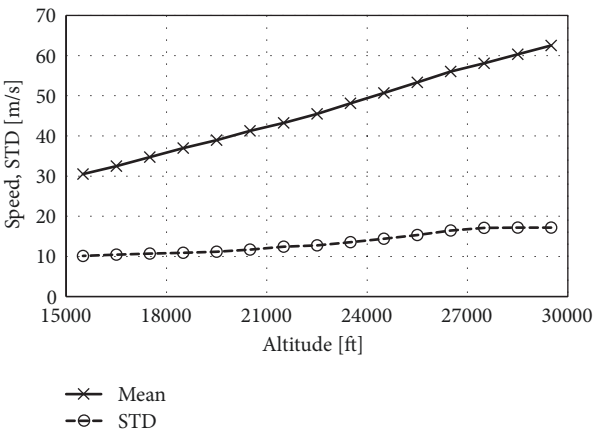

Figure 7: Mean deviation and STD of the tailwind speed.

4. Arrival Time Control Window Model

Based on the IAS distribution shown in Figure 3, it was supposed that the maximum and minimum operational IASs were 320 kt and 230 kt in this study. The arrival time also depends on the tailwind speed. In this study, the mean deviation and STD of the tailwind speed were analyzed, and the average and faster/slower tailwind cases were considered in the numerical investigations. The mean deviation and STD of the tailwind for every 1,000 ft of altitude are summarized in Figure 7. To evaluate the flight time between the initial and terminal points while maintaining the constant IAS of 230 kt or 320 kt, the GS was calculated as the sum of the tailwind and TAS translated from the IAS using the average temperature and pressure. The flight time profile of the cases of 230 kt IAS and 320 kt IAS are shown in Figure 8. The difference between the flight times of these trajectories can be regarded as the arrival time control window. In this study, the nominal trajectory was supposed to have the same reducible and extensible times to arrive at the terminal point. In the average wind case, the arrival time control window, equal to half the difference between the reducible and extensible times, became approximately 60 s to arrive at the terminal starting from the initial point. When the tailwind was slower or faster than the average value, the arrival time control window became larger or smaller, respectively. The arrival

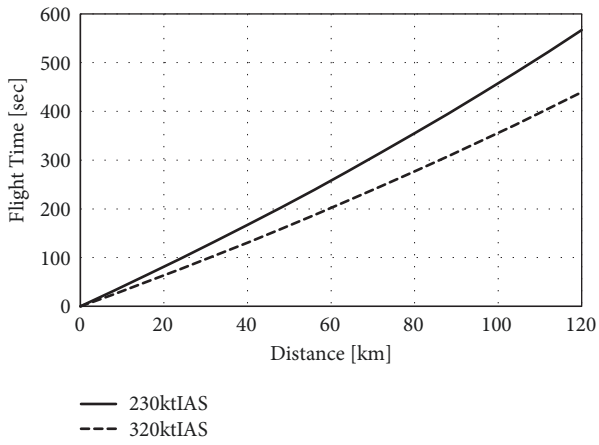

Figure 8: Flight time profiles to the terminal point.

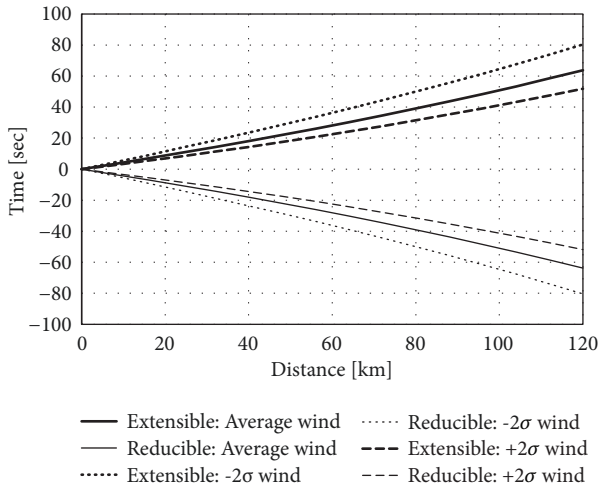

Figure 9: Arrival time control window models.

time control window became a function of the flight distance, which was numerically obtained as follows for the cases with the average and ±2σ wind:

$$t^{ext}(D) = t^{red}(D) = \begin{cases} 1.03 \times 10^{-9} D^2 + 5.44 \times 10^{-4} D\,[\text{sec}] & -2\sigma\ Wind \\ 9.97 \times 10^{-10} D^2 + 4.10 \times 10^{-4} D\,[\text{sec}] & Average\ Wind \\ 9.25 \times 10^{-10} D^2 + 3.20 \times 10^{-4} D\,[\text{sec}] & +2\sigma\ Wind \end{cases} \quad (5)$$

These functions are also shown in Figure 9.

5. Feasibility of Waypoint Position Optimization

To clarify the feasibility of waypoint optimization, the introduction of only one waypoint was considered, and the flight time uncertainty at the terminal point was evaluated by changing its position. For clarity in the investigation, it was assumed that deceleration and acceleration occurred instantaneously and that the flight time error followed a normal distribution based on the central limit theorem.

As was demonstrated in the previous section, the flight time uncertainty increased in proportion to the flight distance. The distribution of the flight time error at the waypoint became like that shown in Figure 10(a). In this case, the aircraft could cancel the flight time error between the arrival time control window before arriving at the terminal point and the flight time error distribution reduced to become like that shown in Figure 10(b). Simultaneously, the flight time uncertainty shown in Figure 10(c) again increased in proportion to the distance to the terminal point. Then the flight time uncertainty was obtained as the sum of the STDs of these distributions. The flight time error distribution at the terminal point is shown in Figure 10(d). Thus, it is possible to estimate the arrival time uncertainty at the terminal point using the models of the flight time uncertainty and arrival time control window.

As was expected from the above example, the arrival time uncertainty at the terminal point became the function of the metering waypoint position. Provided that the flight time followed a normal distribution, the STD of the arrival time at the terminal point was calculated as follows:

$$STD_{terminal} = \left(\int_{-\infty}^{0} t^2 f\left(t - t^{ext}(D_{WP})\right) dt + \int_{0}^{\infty} t^2 f\left(t + t^{red}(D_{WP})\right) dt \right)^{1/2} + \sigma\left(D_{terminal} - D_{WP}\right), \quad (6)$$

where

$$f(t) = \frac{1}{\sqrt{2\pi\sigma^2(D_{WP})}} \exp\left(-\frac{t^2}{2\sigma^2(D_{WP})}\right), \quad (7)$$

and D_{WP} and $D_{terminal}$ are the positions of the waypoint and terminal point, respectively.

The behaviors of the STD at the terminal point in the cases of the average and +2σ and -2σ wind are summarized in Figure 11. It was found that the optimum waypoint position became slightly closer to the terminal point from the middle position of 60 km. It was also found that the optimum waypoint position became closer to the terminal point, and the optimum accuracy became better as the arrival time control window became larger. It is considered that it is more preferable for the arrival time control with a smaller control window to cancel the flight time error at the earlier position where its STD is still sufficiently small for the small control window. By contrast, when the control window was larger, the optimum waypoint position became later to minimize the flight distance to increase the flight time error uncertainty. Thus, the feasibility of waypoint optimization for arrival time accuracy improvement has been clearly demonstrated. However, its effectiveness seems only a little better compared with the case of the middle waypoint placement.

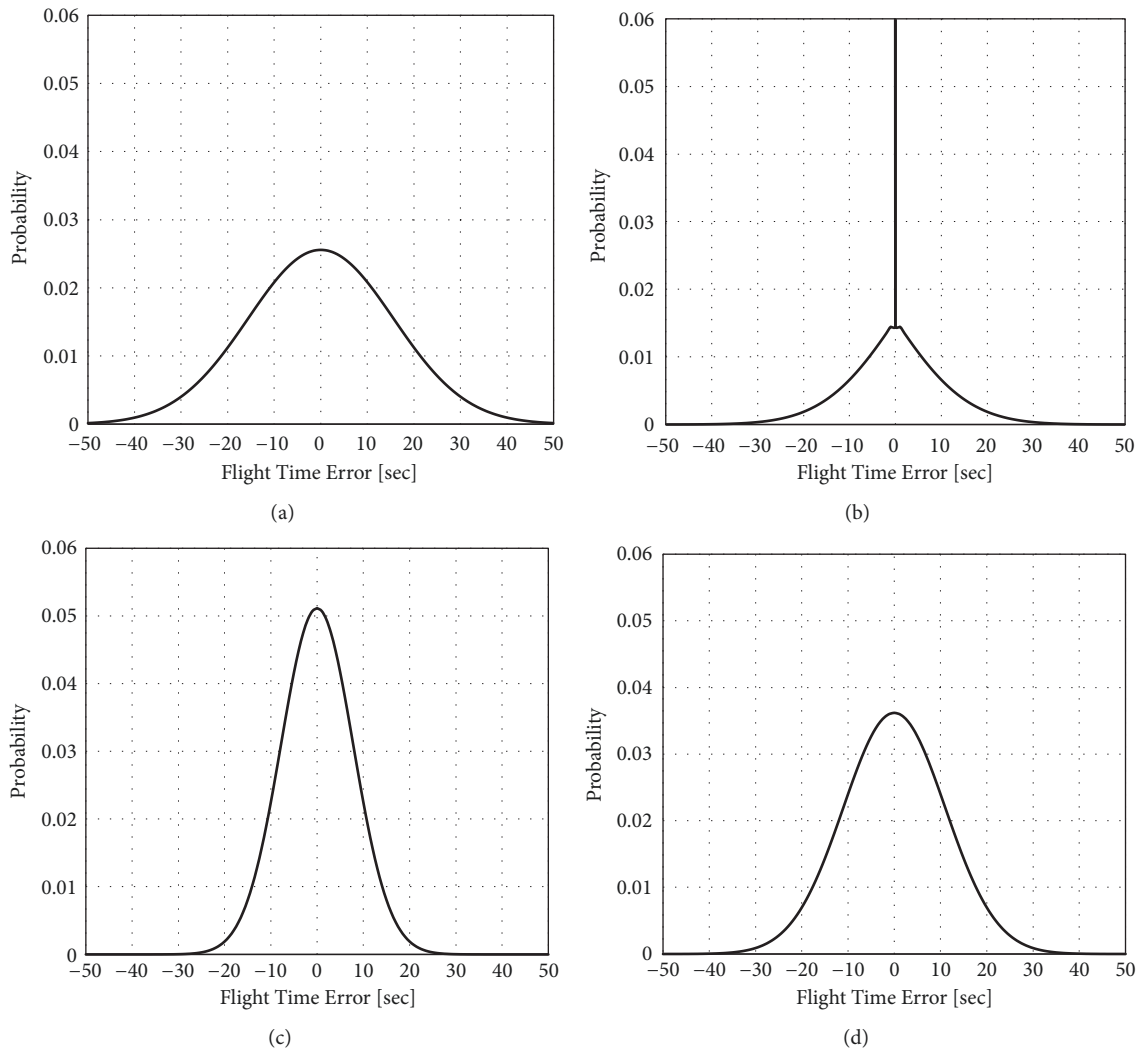

Figure 10: Transition of the flight time error distribution: (a) distribution at the waypoint; (b) reduced distribution at the terminal point after arrival time control; (c) distribution increase from the waypoint to the terminal point; and (d) distribution finally obtained at the terminal point.

6. Position Optimization of Multiple Waypoints

To investigate the effectiveness of multiple waypoints, it is necessary to formulate a nonlinear optimization problem. The objective function is the STD estimated at the terminal point. This becomes a function of the number and positions of the waypoint expressed as follows:

$$\min \quad STD_{terminal}\left(D_1, D_2, \cdots D_N\right), \tag{8}$$

where the STD obeys the following nonlinear recurrence relation:

$$STD_{i+1} = \left(\int_{-\infty}^{0} t^2 f_i\left(t - t^{ext}\left(D_{i+1} - D_i\right)\right) dt + \int_{0}^{\infty} t^2 f_i\left(t + t^{red}\left(D_{i+1} - D_i\right)\right) dt \right)^{1/2} + \sigma\left(D_{i+1} - D_i\right), \tag{9}$$

$$f_i(t) = \frac{1}{\sqrt{2\pi STD_i^2}} \exp\left(-\frac{t^2}{2STD_i^2}\right) \tag{10}$$

subject to the following constraints:

$$0 < D_1 < D_2 < \cdots < D_N < D_{terminal}. \tag{11}$$

Because the objective function in this formulation is nonlinear, sequential quadratic programming [29] was applied for its optimization analysis, where the multistart method was used to avoid local minimum solutions. The optimization results are summarized in Figure 12, which shows the STD at the terminal point by applying the evenly and optimum placed multiple waypoints with the control windows of the average and -2σ wind conditions. The horizontal axis shows the number of waypoints between the initial and terminal points. It is clear that the optimized placement of the waypoints reduced the STD, and that the STD reduction rate became larger as the number of waypoints increased. It

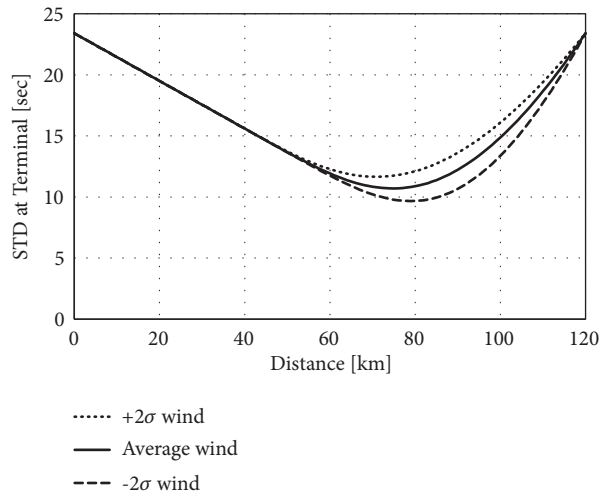

Figure 11: Arrival time STD at the terminal point.

was also clarified that a larger control window enhanced the accuracy in the optimized waypoint cases, whereas a larger control window rarely contributed to the STD reduction in the evenly placed cases. The even and optimized waypoint placements are summarized in Figure 13. The optimized waypoint was placed backward compared with the even waypoint. To investigate this in detail, the history of the STD is summarized in Figure 14, where the horizontal axis shows the distance and the vertical axis shows the STD at each waypoint. Whereas the STD at the evenly placed waypoints remained almost constant, the optimized waypoints were placed closely in the latter part of the trajectory to minimize the STD at the terminal point despite the fact that the STD in the former part of the trajectory once increased larger than that of the evenly placed waypoints case. These characteristics were enhanced when the arrival time control windows increased.

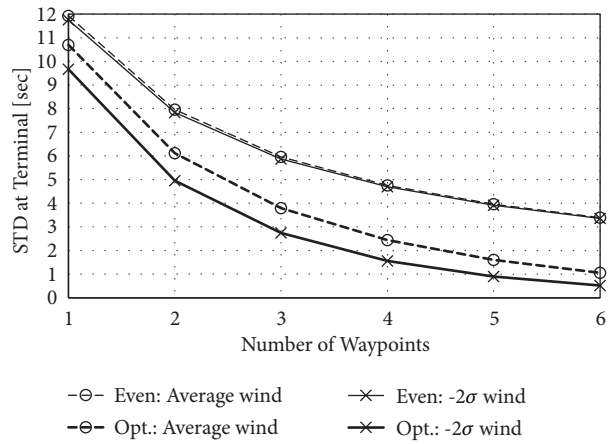

Figure 12: Arrival time STD at the terminal point with multiple waypoints.

7. Conclusion

The feasibility of waypoint optimization for the ground-based arrival time control operation and its effectiveness were investigated using flight time uncertainty and arrival time control window models developed using actual track data and weather forecast data. In this study, the STD at the terminal point was considered as the objective function of the optimization. The feasibility and basic characteristics of the waypoint optimization were demonstrated through analysis using one waypoint. To enhance its effectiveness for accuracy improvement at the terminal point, the application of multiple waypoints and the effect of the arrival time control window were numerically investigated. It was clarified that the simultaneous applications of multiple waypoints and the optimization of the waypoint position achieved a significant improvement of arrival time accuracy. It was also clarified that its effectiveness was enhanced when a larger arrival time control window was applied. From this result, it is expected that the waypoint optimization for arrival time accuracy improvement will become more effective when a more accurate trajectory prediction becomes available. Additionally, it is considered that the optimum waypoint placement also depends on the wind condition that determines the arrival time control window. It must be noted that the accuracy of the flight time uncertainty model is essential in this study. Further investigations of the uncertainty model are necessary.

In this fundamental study on waypoint optimization, many assumptions were made, for example, no difference among aircraft types, the trajectory prediction and control error independent of the weather condition, the normal distribution of the flight time error based on the central limit theorem, and instantaneous speed change. Additionally, only the case in which the nominal trajectory had the same reducible and extensible times to arrive at the terminal point was investigated to clarify the fundamental characteristics. For practical use, these assumptions must be mitigated, and various practical cases must be investigated in detail in future work. Although the flight trajectory considered in this study

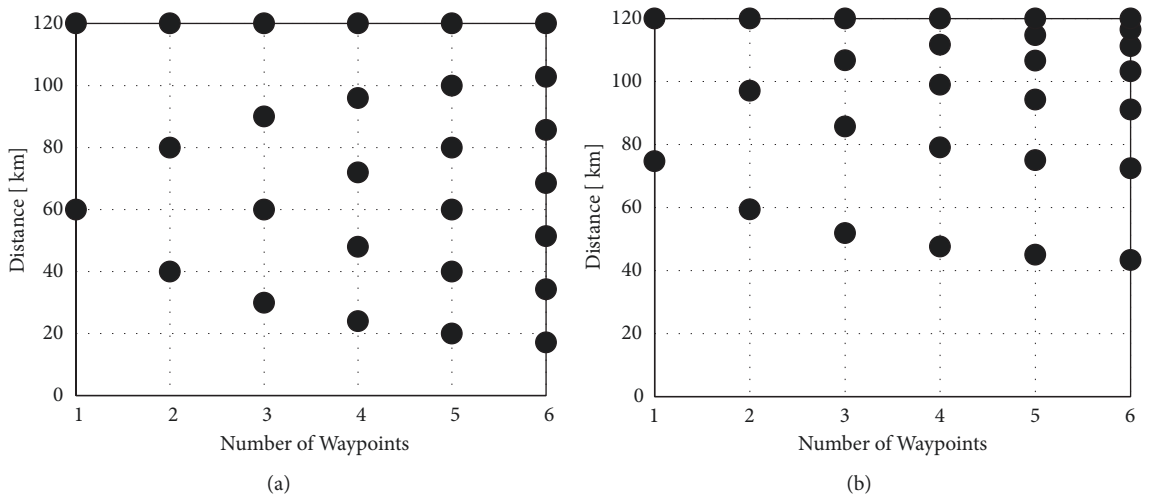

Figure 13: Placement of multiple waypoints: (a) even placement and (b) optimized placement.

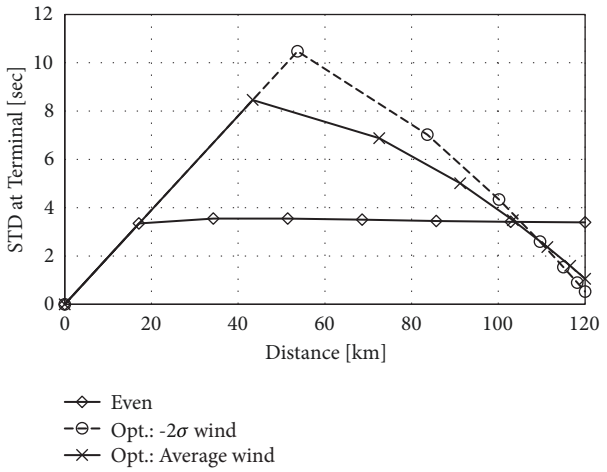

Figure 14: History of the arrival time STD.

is just a part of a descent trajectory, because of the limitation of the available track data, the fundamental characteristics found in this study will also be applicable to the entire trajectory. Because the effectiveness of waypoint optimization will be enhanced in longer trajectories, some investigations on its application to cruise trajectories are necessary to demonstrate its worthiness for practical use. Furthermore, the concept of arrival time uncertainty management presented in this study is considered applicable to the time-based operation using RTA functionality, for example, the waypoint placement to minimize the possibility that the arrival time required from the ATC goes out from the ETA window of the RTA functionality.

Conflicts of Interest

The author declares no conflicts of interest.

References

[1] NextGen Joint Planning and Development Office, *Concept of Operations for the Next Generation Air Transportation System, Version 3.2*, JPDO, Washington, Wash, USA, 2011.

[2] SESAR Joint Undertaking, *Roadmap for Sustainable Air Traffic Management, European ATM Master Plan*, 2nd edition, 2012.

[3] *Long-term Vision for the Future Air Traffic Systems*, l Aviation Bureau, 2010.

[4] H. Erzberger and W. Nedell, "Design of automated system for management of arrival traffic," *NASA TM*, Article ID 102201, 1989.

[5] H. Erzberger, "Design Principles and Algorithms for Automated Air Traffic Management , Knowledge-based Functions in Aerospace Systems," *AGARD Lecture Series*, vol. 200, 1995.

[6] D. De Smedt and G. Berz, "Study of the required time of arrival function of current FMS in an ATM context," in *Proceedings of the 2007 IEEE/AIAA 26th Digital Avionics Systems Conference*, pp. 1.D.5-1–1.D.5-10, Dallas, TX, USA, October 2007.

[7] EUROCONTROL, *Remotely Piloted Aircraft Systems (RPAS) ATM Concept of Operations (CONOPS)*, 4th edition, 2017.

[8] P. Kopardekar, J. Rios, T. Prevot, M. Johnson, J. Jung, and J. E. Robinson, "Unmanned aircraft system traffic management (UTM) concept of operations," in *Proceedings of the 16th AIAA Aviation Technology, Integration, and Operations Conference, 2016*, usa, June 2016.

[9] J.-P. B. Clarke, N. T. Ho, E. Ren et al., "Continuous descent approach: Design and flight test for Louisville international airport," *Journal of Aircraft*, vol. 41, no. 5, pp. 1054–1066, 2004.

[10] R. A. Coppenbarger, R. W. Mead, and D. N. Sweet, "Field evaluation of the tailored arrivals concept for datalink-enabled continuous descent approach," *Journal of Aircraft*, vol. 46, no. 4, pp. 1200–1209, 2009.

[11] T. Callantine, E. Palmer, and M. Kupfer, "Human-in-the-loop simulation of trajectory-based terminal-area operations," in *Proceedings of the 27th International Congress of the Aeronautical Sciences*, Nice, France, 2010.

[12] R. Coppenbarger, G. Dyer, M. Hayashi, R. Lanier, L. Stell, and D. Sweet, "Development and testing of automation for efficient

arrivals in constrained airspace," in *Proceedings of the 27th Congress of the International Council of the Aeronautical Sciences 2010, ICAS 2010*, pp. 4058–4071, fra, September 2010.

[13] J. E. Robinson, J. Thipphavong, and W. C. Johnson, "Enabling performance-based navigation arrivals:development and simulation testing of the terminal sequencing and spacing system," in *Proceedings of the 11th USA/Europe Air Traffic Management Research and Development Seminar, ATM 2015*, prt, June 2015.

[14] J. Kaneshige, S. Sharma, L. Martin, S. Lozito, and V. Dulchinos, "Flight-deck strategies and outcomes when flying schedule-matching descents," in *Proceedings of the AIAA Guidance, Navigation, and Control (GNC) Conference*, usa, August 2013.

[15] T. J. Callantine, M. Kupfer, L. Martin, and T. Prevot, "Simulations of continuous descent operations with arrival-management automation and mixed flight-deck interval management equipage," in *Proceedings of the 10th USA/Europe Air Traffic Management Research and Development Seminar, ATM 2013*, usa, June 2013.

[16] L. Boursier, B. Favennec, E. Hoffman, A. Trzmiel, F. Vergne, and K. Zeghal, "Merging arrival flows without heading instructions," in *Proceedings of the 7th USA/Europe Air Traffic Management Research and Development Seminar, ATM 2007*, pp. 414–421, esp, July 2007.

[17] B. Barmore, W. Capron, T. Abbott, and B. Baxley, "Simulation Results for Airborne Precision Spacing along Continuous Descent Arrivals," in *Proceedings of the The 26th Congress of ICAS and 8th AIAA ATIO*, Anchorage, Alaska.

[18] H. N. Swenson, J. Thipphavong, A. Sadovsky, L. Chen, C. Sullivan, and L. Martin, "Design and evaluation of the terminal area precision scheduling and spacing system," in *Proceedings of the 9th USA/Europe Air Traffic Management Research and Development Seminar, ATM 2011*, pp. 158–167, deu, June 2011.

[19] M. Kupfer, T. Callantine, L. Martin, J. Mercer, and E. Palmer, "Controller support tools for schedule-based terminal-area operations," in *Proceedings of the 9th USA/Europe Air Traffic Management Research and Development Seminar, ATM 2011*, pp. 516–525, deu, June 2011.

[20] J.-P. Clarke, J. Brooks, G. Nagle, A. Scacchioli, W. White, and S. R. Liu, "Optimized profile descent arrivals at Los Angeles international airport," *Journal of Aircraft*, vol. 50, no. 2, pp. 360–369, 2013.

[21] P. M. de Jong, F. J. Bussink, R. P. Verhoeven, N. de Gelder, M. M. van Paassen, and M. Mulder, "Time and Energy Management During Approach: A Human-in-the-Loop Study," *Journal of Aircraft*, vol. 54, no. 1, pp. 177–189, 2017.

[22] J. Bronsvoort, G. McDonald, R. Potts, and E. Gutt, "Enhanced descent wind forecast for aircraft," in *Proceedings of the 9th USA/Europe Air Traffic Management R&D Seminar*, Berlin, Germany.

[23] J. López Leonés, A. D. Amo, J. Bronsvoort et al., "Air-Ground Trajectory Synchronization through Exchange of Aircraft Intent Information," *Air Traffic Control Quarterly*, vol. 20, no. 4, pp. 311–339, 2012.

[24] J. Bronsvoort, G. McDonald, M. Vilaplana, and J. A. Besada, "Two-stage approach to integrated air/ground trajectory prediction," *Journal of Guidance, Control, and Dynamics*, vol. 37, no. 6, pp. 2035–2039, 2014.

[25] ICAO, *Manual on the Secondary Surveillance Radar (SSR) Systems*, Doc.9684AN/951, 3rd edition, 2004.

[26] A. Senoguchi and T. Koga, "Analysis of downlink aircraft parameters monitored by SSR Mode S in ENRI," in *Proceedings of the 28th Digital Avionics Systems Conference: Modernization of Avionics and ATM-Perspectives from the Air and Ground, DASC 2009*, pp. 4.D.41–4.D.49, usa, October 2009.

[27] Y. Honda, M. Nishijima, K. Koizumi et al., "A pre-operational variational data assimilation system for a non-hydrostatic model at the Japan Meteorological Agency: Formulation and preliminary results," *Quarterly Journal of the Royal Meteorological Society*, vol. 131, no. 613, pp. 3465–3475, 2006.

[28] A. Nuic, *User Manual for the Base of Aircraft Data (BADA) Revision 3.11*, Eurocontrol Experimental Center, 2013.

[29] J. Nocedal and S. J. Wright, *Numerical Optimization*, Springer, New York, NY, USA, 2006.